

2010

Ancient DNA Analyses Exclude Humans as the Driving Force Behind Late Pleistocene Musk Ox (*Ovibos moschatus*) Population Dynamics

Paula F. Campos

Eske Willerslev


Andrei Sher

Ludovic Orlando

Erik Axelsson

See next page for additional authors

Follow this and additional works at: https://digitalcommons.odu.edu/biology_fac_pubs

 Part of the [Climate Commons](#), [Genetics Commons](#), [Paleobiology Commons](#), and the [Paleontology Commons](#)

Repository Citation

Campos, Paula F.; Willerslev, Eske; Sher, Andrei; Orlando, Ludovic; Axelsson, Erik; Tikhonov, Alexei; Aaris-Sorensen, Kim; Greenwood, Alex D.; Kahlke, Ralf-Dietrich; and Kosintsev, Pavel, "Ancient DNA Analyses Exclude Humans as the Driving Force Behind Late Pleistocene Musk Ox (*Ovibos moschatus*) Population Dynamics" (2010). *Biological Sciences Faculty Publications*. 285. https://digitalcommons.odu.edu/biology_fac_pubs/285

Original Publication Citation

Campos, P. F., Willerslev, E., Sher, A., Orlando, L., Axelsson, E., Tikhonov, A., . . . Gilbert, M. T. P. (2010). Ancient DNA analyses exclude humans as the driving force behind late pleistocene musk ox (*Ovibos moschatus*) population dynamics. *Proceedings of the National Academy of Sciences of the United States of America*, 107(12), 5675-5680. doi:10.1073/pnas.0907189107

Authors

Paula F. Campos, Eske Willerslev, Andrei Sher, Ludovic Orlando, Erik Axelsson, Alexei Tikhonov, Kim Aaris-Sorensen, Alex D. Greenwood, Ralf-Dietrich Kahlke, and Pavel Kosintsev

Ancient DNA analyses exclude humans as the driving force behind late Pleistocene musk ox (*Ovibos moschatus*) population dynamics

Paula F. Campos^a, Eske Willerslev^a, Andrei Sher^{b,1}, Ludovic Orlando^c, Erik Axelsson^a, Alexei Tikhonov^d, Kim Aaris-Sørensen^a, Alex D. Greenwood^{e,2}, Ralf-Dietrich Kahlke^f, Pavel Kosintsev^g, Tatiana Krakhmalnaya^h, Tatyana Kuznetsovaⁱ, Philippe Lemeij^j, Ross MacPhee^k, Christopher A. Norris^l, Kieran Shepherd^m, Marc A. Suchardⁿ, Grant D. Zazula^o, Beth Shapiro^p, and M. Thomas P. Gilbert^{a,3}

^aCentre for GeoGenetics, Natural History Museum of Denmark, University of Copenhagen, DK 1350 Copenhagen, Denmark; ^bSvertsov Institute of Ecology and Evolution, Russian Academy of Sciences, Moscow 119071, Russia; ^cPaleogenetics and Molecular Evolution, Institut de Génétique Fonctionnelle de Lyon, Université de Lyon, Université Lyon 1, Centre National de la Recherche Scientifique, Institut National de la Recherche Agronomique, Ecole Normale Supérieure de Lyon, 69364 Lyon Cedex 07, France; ^dZoological Institute, Russian Academy of Sciences, St. Petersburg 199034, Russia; ^eDepartment of Biological Sciences, Old Dominion University, Norfolk, VA 23529; ^fSenckenberg Research Institutes and Natural History Museums, Research Station of Quaternary Palaeontology, D-99423 Weimar, Germany; ^gInstitute of Plant and Animal Ecology, Urals Branch of the Russian Academy of Sciences, Ekaterinburg 620144, Russia; ^hNational Museum of Natural History, National Academy of Sciences of Ukraine, Kiev 01030, Ukraine; ⁱDepartment of Paleontology, Faculty of Geology, Lomonosov Moscow State University, Moscow 119991, Russia; ^jDepartment of Microbiology and Immunology, Rega Institute, Katholieke Universiteit Leuven, B-3000 Leuven, Belgium; ^kDivision of Vertebrate Zoology, American Museum of Natural History, New York, NY 10024; ^lDivision of Vertebrate Paleontology, Peabody Museum of Natural History, New Haven, CT 06520; ^mCollections, Canadian Museum of Nature, Ottawa, ON K1P 6P4, Canada; ⁿDepartment of Biomathematics, Department of Biostatistics, and Department of Human Genetics, University of California, Los Angeles, CA 90095; ^oYukon Palaeontology Program, Department of Tourism and Culture, Yukon Government, Whitehorse, YT Y1A 2C6, Canada; and ^pDepartment of Biology, Pennsylvania State University, University Park, PA 16801

Edited by David J. Meltzer, Southern Methodist University, Dallas, TX, and approved February 1, 2010 (received for review June 27, 2009)

The causes of the late Pleistocene megafaunal extinctions are poorly understood. Different lines of evidence point to climate change, the arrival of humans, or a combination of these events as the trigger. Although many species went extinct, others, such as caribou and bison, survived to the present. The musk ox has an intermediate story: relatively abundant during the Pleistocene, it is now restricted to Greenland and the Arctic Archipelago. In this study, we use ancient DNA sequences, temporally unbiased summary statistics, and Bayesian analytical techniques to infer musk ox population dynamics throughout the late Pleistocene and Holocene. Our results reveal that musk ox genetic diversity was much higher during the Pleistocene than at present, and has undergone several expansions and contractions over the past 60,000 years. Northeast Siberia was of key importance, as it was the geographic origin of all samples studied and held a large diverse population until local extinction at $\approx 45,000$ radiocarbon years before present (^{14}C YBP). Subsequently, musk ox genetic diversity reincreased at ca. 30,000 ^{14}C YBP, recontracted at ca. 18,000 ^{14}C YBP, and finally recovered in the middle Holocene. The arrival of humans into relevant areas of the musk ox range did not affect their mitochondrial diversity, and both musk ox and humans expanded into Greenland concomitantly. Thus, their population dynamics are better explained by a nonanthropogenic cause (for example, environmental change), a hypothesis supported by historic observations on the sensitivity of the species to both climatic warming and fluctuations.

climate change | human impact | quaternary | megafauna extinctions

The late Pleistocene saw significant changes in the geographic distribution and composition of the Beringian megafauna. Although many iconic Beringian herbivores, such as mammoths (*Mammuthus primigenius*) and woolly rhinoceroses (*Coelodonta antiquitatis*) became extinct, others, such as horses (*Equus caballus*), saiga (*Saiga tatarica*), caribou (*Rangifer tarandus*), and bison (*Bison bison*) survived to the present. The reasons for these markedly different survival patterns have been widely debated, with the extinctions predominantly attributed to either human impact (1) or climate change associated with the last glacial cycle (2). The relative contribution of the two remains a key evolutionary debate (cf. 3, 4). For example, it is well known that global climate fluctuated significantly throughout the

Pleistocene (5–7); the Eurasian fossil record indicates that late Pleistocene climatic changes reduced the range of several species, and the last glacial-interglacial transition appears to correlate with major extinction events. However, none of the previous Pleistocene glacial cycles appear to have caused widespread extinction events (3, 8), and the demise of the Beringian megafauna also appears to coincide neatly with the arrival and spread of modern human populations (9, 10). Similar evidence of a human-driven effect can be seen in central North America, where the arrival of Clovis-style hunters, extinction of megafauna, and marked climate change all cluster closely together (11, 12).

Ancient DNA (aDNA) analyses of temporally and geographically distributed megafaunal remains offer a means to address the relative roles of humans versus the climate in the Beringian megafaunal extinctions. The capacity of this technique to detect changes in genetic diversity within populations over geologically significant time scales provides the means to examine past population variation and to explore directly how populations respond to climate and environmental changes (13). Geographic and temporal discontinuity in the genetic data can be compared to past climate reconstructions and specific ecological events, such as advancing ice sheets, a volcanic eruption, or human colonization. Previous large-scale aDNA studies of this kind have focused on herbivores, such as bison and horses that survived to the present in relatively large numbers and are thus relatively

Author contributions: P.F.C., E.W., A.S., B.S., and M.T.P.G. designed research; P.F.C. and M.T.P.G. performed research; E.W., A.S., A.T., K.A.-S., A.G., R.-D.K., P.K., T. Krakhmalnaya, T. Kuznetsova, R.M., C.A.N., K.S., M.A.S., G.D.Z., and M.T.P.G. contributed new reagents/analytic tools; P.F.C., E.W., A.S., L.O., E.A., P.L., B.S., and M.T.P.G. analyzed data; and P.F.C., L.O., E.A., A.T., K.A.-S., A.G., R.-D.K., P.K., T. Krakhmalnaya, T. Kuznetsova, P.L., R.M., C.A.N., K.S., M.A.S., G.D.Z., B.S., and M.T.P.G. wrote the paper.

The authors declare no conflict of interest.

This article is a PNAS Direct Submission.

Data deposition: Musk Ox DNA sequences are submitted to Genbank under Accession ID numbers GU808088–GU808249.

¹Deceased August 11, 2008.

²Leibniz-Institute for Zoo and Wildlife Research & Faculty of Veterinary Medicine, Freie Universität Berlin, Alfred-Kowalke Str. 17, D-10315 Berlin, Germany.

³To whom correspondence should be addressed. E-mail: mtgilbert@gmail.com.

This article contains supporting information online at www.pnas.org/cgi/content/full/0907189107/DCSupplemental.

abundant today (13, 14), or others, such as the mammoth that are now extinct (15, 16). We focus on the musk ox, *Ovibos moschatus*, one of the few large mammals adapted to a high arctic environment, and which has a distinctly different pattern of survival than the previously studied species. Although the musk ox was holarctically distributed at the beginning of the Holocene, only small, relict natural populations isolated on Greenland and the North American Arctic Archipelago survive to the present day. The Pleistocene musk ox went extinct over most of its Eurasian range at the beginning of the Holocene. In Europe, the latest known occurrences are in late glacial deposits in Scandinavia, and in the Taimyr Peninsula and the Lena River mouth at the Bykovsky Peninsula (Northeast Siberia) they survived until around 2,500 years before present (YBP) (17, 18), extending the survival of this species in northern Russia well into the Holocene epoch.

Whether musk ox population decline can be attributed to human or other effects is unclear. In North America, the decline of related ovibovines appears to correlate closely with the arrival of humans, whereas longer human-ovibovine cohabitation is observed in northern Eurasia (3, 19). Given the conflicting evidence, a principal aim of this study was to further investigate the question, through reconstruction of past musk ox population dynamics using aDNA, and comparison of the findings against human and climatic records from the late Pleistocene and Holocene and known biological characteristics of the species.

Results and Discussion

To investigate changes in genetic diversity among musk ox since the late Pleistocene, we analyzed 682 bp of the mitochondrial control region, obtained from 149 radiocarbon dated specimens that range in age from 56,900 radiocarbon (^{14}C) YBP to the present (Fig. 1). Specimens were sampled from their previous geographic range, spanning from the Urals ($n = 26$) and the Taimyr Peninsula ($n = 54$) in the west, through Northeast Siberia ($n = 12$) and into North America ($n = 14$) and across to Greenland ($n = 43$) in the east. Our data demonstrate continuous

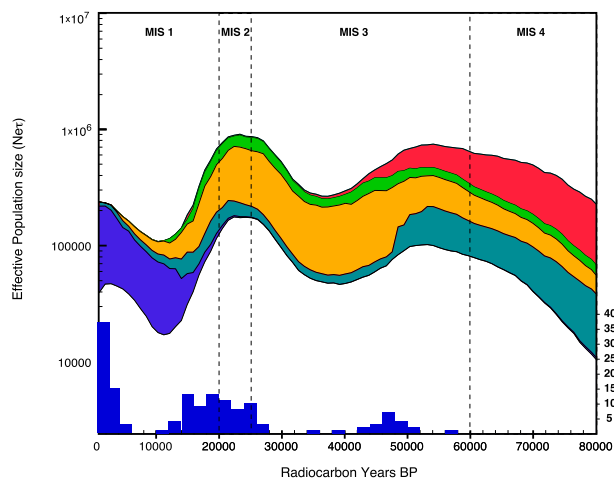


Fig. 1. Bayesian Skyride derived from the geospatial analysis of 135 ancient and 14 modern musk ox mtDNA control region sequences. The x axis is in units of radiocarbon years in the past, and the y axis is equal to $Ne^*\tau$ (the product of the effective population size and the generation length in radiocarbon years). The colors represent the relative contribution of each of the geolocations to the overall estimated effective population size. Colors indicate geographical origins of the samples: blue, Greenland; red, Northeast Siberia; orange, Taimyr; green, Urals; light blue, Canada. The bar graph shows the number of radiocarbon-dated samples in bins of 2,000 radiocarbon years. No relation is apparent between the absolute number of samples and the estimated effective population size or transition time.

presence of musk ox in Eurasia and North America throughout radiocarbon time until their extinction in Eurasia ($\sim 2,500$ YBP) and demographic retraction in North America ($\sim 10,000$ YBP).

Loss of Mitochondrial DNA Diversity. Modern musk ox harbor little genetic diversity at both the nuclear and mitochondrial levels (20–22). Our data indicate that total past genetic diversity (samples older than 100 ^{14}C YBP), as measured by temporally unbiased π (23), was significantly higher than present (Table 1 and Fig. S1), with Serial SimCoal (SSC) simulations indicating that this decrease in genetic diversity cannot be explained by genetic drift in a constant-sized population. This observation is consistent with the results of a smaller, previous aDNA study (24) and with paleontological evidence, which suggests a large decrease in musk ox geographic range and population size during the late Pleistocene. To investigate whether the arrival of humans into the musk ox range played any effect on the species' genetic diversity, a similar analysis was performed on the Taimyr and Canada datasets (the only two with a meaningful number of musk ox on either side of the entry). In neither case was human arrival associated with any statistically significant change in genetic diversity (Table 1 and Fig. S1).

Three Geographically Structured Clades. Phylogenetic analyses of the data subdivides musk ox into three, well-supported and temporally structured clades (clades 1–3) (Fig. 2). The phylogeny is consistent with that recovered when (i) 13 radiocarbon-infinite sequences are added to the alignment, or (ii) the analysis is restricted to a subset of 60 samples for which the complete control region sequence was obtained (Figs. S2 and S3). Clade 1 comprises samples that range in age from beyond the ^{14}C limit to 42,550 ^{14}C YBP, originating predominantly in Northeast Siberia but also in the Taimyr Peninsula. By $\approx 45,000$ ^{14}C YBP, most of the diversity present before this time had been lost.

Clade 2 consists of specimens almost exclusively originating from the Urals and Taimyr region, ranging in age from beyond the ^{14}C limit to ca. 13,000 ^{14}C YBP (although a single outlier in this study is associated with a much more recent date of 3374 ^{14}C YBP). The geographic distribution of samples belonging to clade 2 suggests: (i) that these regions were either independently populated from a mixed source population, (ii) that no significant physical barriers to gene flow were present across this wide geographic expanse, or (iii) a combination of these. During the Quaternary, ice sheets over the Barents and Kara seas expanded several times onto mainland Russia, blocking north-flowing rivers such as the Yenisei, Ob, Pechora, and Mezen. Large ice-dammed lakes formed a barrier

Table 1. Observed nucleotide diversity and polymorphic sites of data subsets

Data subset	π^*	Significance [†]	M	PM
All modern samples (<100 ^{14}C YBP)	0.008	6,417	26	9
All ancient samples (>100 ^{14}C YBP)	0.021	9,993 [‡]	575	549
Canada, prehuman contact [§]	0.026	4,801	70	Na
Canada posthuman contact [§]	0.019	6,689	45	Na
Taimyr prehuman contact [§]	0.025	4,006	136	Na
Taimyr posthuman contact [§]	0.017	6,815	39	Na

M, number of polymorphic sites; Na, Not applicable; PM, number of private mutations.

*Temporally unbiased π calculated following Depaulis et al. (23).

[†]Rank (of 10,000, of uncorrected π) among data generated through Serial SimCoal simulations of a constant population in which gene frequencies are changing only through genetic drift. Placement of the observed value outside of the 95th percentile (i.e., outside of rank 250–9,750) can be considered as significant at <5% level.

[‡]Significant at $P = 0.0007$.

[§]Contact time as shown in Fig. 3.

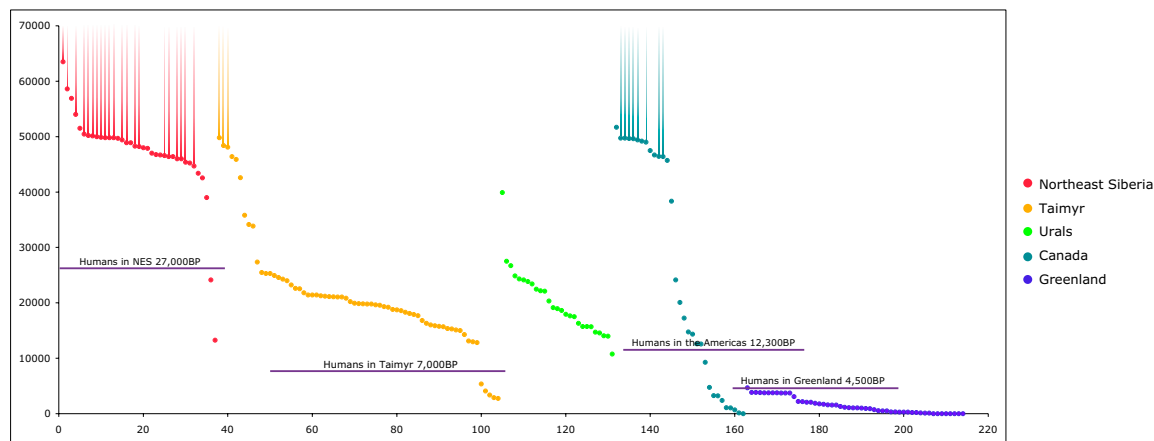


Fig. 3. Temporal distribution of the 210 ^{14}C dated fossil musk ox used in the present study. For a number of individuals, indicated by the extended timelines, finite dates could not be calculated. Samples are grouped in five major regions: Northeast Siberia, Taimyr, Urals, Canada, and Greenland. The approximate earliest presence of anatomically modern humans in the regions is added for comparison. Radiocarbon accession numbers associated with specific specimens are given in Table S1.

The periods during which musk ox populations are seen to increase are, in general, those of global climatic cooling (in particular as peak diversity coincides with the LGM). Furthermore, the musk ox populations decline during the warmer and climatically unstable interstadials (Fig. S6), such as MIS 3, and in the postglacial warming following the LGM (Fig. 1 and Fig. S7). Although this is by no means conclusive evidence, a role of the environment as opposed to humans as the driving force is also supported by several other observations drawn from both our, and previously published data, as discussed below.

The results of the geospatial analyses point to a significant role of Northeast Siberia in the species' population history. This region not only harbored the greatest mitochondrial genetic diversity, but also the most recent common ancestor of all sampled musk ox [$\approx 96,009$ years ago (95% highest posterior density [HPD] 103,249–82,780 years ago)] and was the geographic source of all three clades. Despite its key role in musk ox history, both the time of extinction of clade 1 and the temporal distribution of the ^{14}C dated specimens (Figs. 2 and 3) indicate that a major reduction in musk ox diversity occurred in this region at ca. 45,000 ^{14}C YBP. There is no archaeological evidence of human presence this far north at this time; the first well-supported evidence of human settlements in Northeast Siberia are at a Paleolithic site in the Yana River basin at 27,000 ^{14}C YBP (37). Thus, an alternate explanation for the loss is required. Intriguingly, the loss of a distinct mtDNA clade for mammoths has also been observed in this region at this time (15, 16, 38), suggesting the cause was not species-specific. Given that during MIS 3 both polar ice-core records and pollen, plant macrofossils, mammal, and insect remains indicate that the climate started to both fluctuate significantly and become increasingly warmer and wetter (39–41) (Fig. S7), and that, as discussed above, musk ox are sensitive to both climate warming and fluctuations (32, 42), climatic-driven environmental change is a plausible hypothesis.

The distribution of the ^{14}C dated samples in both the Taimyr and Urals indicates a widespread loss of musk ox in these regions following the LGM, culminating by around 13,000 ^{14}C YBP (Fig. 3). There is no evidence for the presence of modern humans in the area until the very end of the Pleistocene or early Holocene (43–45), and as mentioned above, the human arrival in the Taimyr is associated with no statistically significant change in genetic diversity (Table 1). However, this time does coincide with the Bølling/Allerød period, during which the climate became more humid and a general degradation of permafrost started, accompanied by a dramatic change in vegetation from tundra-steppe to wet tundra and forest tundra

(7). Thus, once again, the data directly suggest that these fluctuations were driven by nonanthropogenic factors.

Further evidence of the competing roles of humans versus environment is provided by the Greenlandic data. Although musk ox were present in the Americas throughout the Pleistocene, they did not colonize Greenland until very recently. Although other species, such as caribou, are known to have been present in Greenland during the last interglacial (46), the fossil record shows that musk ox first arrived in Greenland during the mid-Holocene, with the oldest samples dated to 4,500 ^{14}C YBP, from Paleoeskimo Independence I archeological sites in Northeast and Northwest Greenland (47). The fossil record and the modern geographical range of the musk ox suggest that dispersal into Greenland took place from Ellesmere Island in Canada by way of the Robeson Channel to Northwest Greenland, followed by dispersal along the east coast into central East Greenland (48, 49). Our results are consistent with this pattern, and support a single colonization event followed by population expansion.

Bayesian skyline analysis of the restricted Greenlandic dataset suggests rapid population growth following this initial dispersal into Greenland (Fig. S8). This theory is consistent with the expected dynamics of a species entering virgin terrain in the absence of competition and the fact that musk ox thrive during climatically stable periods (42), such as those reconstructed for the last ca. 10,000 years in Greenland using GISP2 records (Fig. S7) (50, 51). This finding, plus the contemporaneous arrival and colonization of Greenland by humans and musk ox, and the fact that musk ox genetic diversity in Canada did not change significantly following human arrival in the Americas (Table 1), provides further evidence of a negligible effect of humans on musk ox. Arguments that musk ox were not of interest to the first humans as prey can also be discounted, as the Independence I culture are known to have been expert musk ox hunters, as demonstrated by the large number of musk ox bones recovered from archeological sites across the high Arctic of Canada and Greenland that have been associated with this culture (52).

In summary, although humans may have played a significant role in the history of other large Beringian mammalian herbivores, to our knowledge this example is unique in showing there is no evidence that humans drove musk ox demographic fluctuations over the last 60,000 years. We argue that an alternate cause, possibly environmental change driven by the climate (53), was the major force behind musk ox population dynamics over this period, and expect that with the arrival of future aDNA and climatic reconstructions, this hypothesis can be more explicitly tested.



Fig. 4. Geographic origin of musk ox samples that yielded aDNA sequences.

Materials and Methods

DNA Extraction and Amplifications. We collected samples from 447 bone, teeth, or horn core-fossil specimens from the North Sea, Ukraine, Urals, Taimyr Peninsula, Northeast Siberia, Alaska, Canada, and Greenland (Fig. 4). Stringent aDNA protocols were followed to avoid contamination from modern DNA and assure reliability of the results. For full details see *SI Materials and Methods* and *Table S2*.

The absence of any clearly identifiable alternative sequence among these clones, coupled with the absence of any mismatch when the heavily overlapping primers in our amplification strategies were used, suggests that nuclear-encoded copies of mitochondrial sequences were not recovered, although they have been obtained from ancient and modern musk ox (54). Sequences were found to be totally consistent between fragments generated by different primer pairs and replicable between amplifications when the same primer pairs were used.

Mitochondrial control region DNA was successfully amplified and sequenced from 216 of 447 specimens (49%), including specimens morphologically identified as *Ovibos moschatus*, *Ovibos pallantis*, and *Praeovibos* sp. For 60 specimens we were able to recover the complete control region sequence. For 162 samples we were able to recover the 682 bp sequence that comprises the main focus of the analyses. For an additional 52 specimens we were only able to amplify part of the 682 bp targeted, and thus they were excluded from the subsequent phylogenetic analyses.

Data Analyses. Phylogenetic relationships among the 162 specimens that yielded 682 bp of sequence were estimated using Bayesian Markov chain Monte Carlo (MCMC) as implemented in the phylogenetic analysis software MrBayes 3.1 (55). In each analysis, four chains (with heating according to default settings) were run for 2 million generations, with parameters written to file every 1,000 generations. Two separate runs of 2 million generations were conducted simultaneously under the best-fit model of molecular evolution (HKY+G) as identified by MODELTEST v3.7 (56). Tracer 1.4 (57) was used to check for stabilization and convergence between runs. The first quarter (25%) of the trees was discarded as burn-in, and the remaining trees were summarized with the majority-rule consensus approach, using posterior probability as a measure of clade support.

Genetic relationships among the dated specimens were estimated using BEAST v1.4.8 (58), with simultaneous estimation of tree topology, evolutionary model parameters, and demographic parameters. The HKY+G nucleotide substitution model was assumed along with the Bayesian skyline plot demographic model (31). Two MCMC chains were run for 50 million iterations, with parameters written to file every 1,000 iterations. Con-

vergence and mixing were evaluated using Tracer (57), and maximum clade credibility trees were compiled from the posterior samples using TreeAnnotator. Separate analyses were performed for the whole dataset, for the Taimyr+Urals clade and for Greenland. A mutation rate of 8.7×10^{-7} was obtained from this dataset (95% HPD: 6.53×10^{-7} to 1.0×10^{-6}).

Previous authors have argued that the presence of postmortem DNA damage-driven lesions (PMD) in ancient DNA sequences may complicate the interpretation of population genetic studies based on aDNA, inflating estimates of diversity (e.g., refs. 59 and 60). To assess for the robustness of the data, several additional analyses were performed. First, the analysis was performed as above; however, also including the PMD model (61), which allows each segregating transition to be the result of postmortem damage rather than evolution within a probabilistic framework. Analyses were performed in BEAST, as described above. Damage levels were shown to be very low (95% HPD: 2.27×10^{-12} and 1.2×10^{-8}). The results of the PMD analysis were not significantly different from those of the analysis excluding the PMD model, and a Bayes factor test (62) indicated that the PMD model provided no improvement of fit over the simpler model (Bayes factor = 8.482, with preference for the analysis without the damage model). Second, as postmortem damage is likely to only be observed as singletons in the dataset, the analysis was also performed on the dataset after removing all singletons. Again, genetic relationships among the dated specimens were estimated using BEAST with evolutionary and coalescent models, as described above. The results do not differ from the previous analysis (with or without PMD) except that the effective population (N_e) size decreased as it was expected because we removed diversity when we discarded the singletons (Fig. S9).

We used SSC (63, 64) to model several aspects of the data (Fig. S10). First, the results of the phylogenetic analysis indicate that the mtDNA phylogenetic structure existed in the musk ox population (Fig. 2), with particular distinction between the Taimyr/Urals individuals, and the rest. As demographic parameters are estimated by BEAST under the assumption of a single population, SSC was used to explore whether the population dynamics recovered in the BEAST analyses (Fig. 1) could arise simply as a consequence of population substructure combined with our sampling strategy. Second, we used SSC to model whether the observed nucleotide (π) diversities of the modern (< 100 ^{14}C YBP), ancient (> 100 ^{14}C YBP), and pre- and posthuman contact samples (from Canada and Taimyr) differed significantly, or could be explained solely as a result of our sampling scheme in a single, constant-sized, population. Full details of the simulations are described in *SI Materials and Methods*.

To assess the geospatial distribution of musk ox through time, an additional BEAST analysis was performed with the full dataset of finite radiocarbon-dated specimens. In this analysis, in addition to the parameters described above, the probability distribution of the geographic locations of each node in the tree were also inferred. Briefly, this discrete geospatial model (65) assigns each sequence to a fixed location in space (here, five locations were assumed: Greenland, Northeast Siberia, Taimyr, Urals, and Canada). Rates of diffusion between each of these sites are then estimated according to a continuous-time Markov chain. Under the continuous-time Markov chain model, the unobserved location at the root of the tree derives from a uniform distribution over all sampled locations. Dispersal then proceeds conditionally independently along each branch in the tree according to a memory-less transition process and ultimately gives rise to the observed locations at the tips. An infinitesimal-rate matrix Q characterizes this Markov model and we estimate these rates from the data using Bayesian stochastic variable selection to achieve statistical efficiency as the data represent only a single realization from the process. The posterior probabilities of a given node in tree existing at each possible location are simultaneously estimated along the tree and evolutionary model in BEAST. This simultaneous inference also assumes the Bayesian skyline plot coalescent prior over the tree and incorporates the PMD model to account for possible damaged sites. Two MCMC chains were run for 100 M iterations, with subsamples recorded from the posterior every 10 K iterations.

ACKNOWLEDGMENTS. The authors thank Jennifer Leonard for useful discussion and A. Cooper, P. Matheus, J. Meng, and D. Mol for access to their collections and obtaining samples. This study was funded in part by Forsknings-og Innovationsstyrelsen 272-07-0279 Skou Grant (to M.T.P.G.) and the Marie Curie Actions "GeneTime" Grant (to P.F.C. and E.W.).

1. Martin PS (1967) Pre-historic over kill. *Pleistocene Extinctions: The Search for a Cause (Proceedings of the VII Congress of the International Association for Quaternary Research)*, eds Martin PS, Wright HE, Yale University Press, New Haven, CT, pp 75–120.

2. Guthrie RD (2006) New carbon dates link climatic change with human colonization and Pleistocene extinctions. *Nature* 441:207–209.

3. Barnosky AD, Koch PL, Feranec RS, Wing SL, Shabel AB (2004) Assessing the causes of Late Pleistocene extinctions on the continents. *Science* 306:70–75.

4. Faith J, Surovell T (2009) Synchronous extinction of North America's Pleistocene mammals. *Proc Natl Acad Sci USA* 106:20641.
5. Svendsen JJ, et al. (2004) Late Quaternary ice sheet history of northern Eurasia. *Quat Sci Rev* 23:1229–1271.
6. Andreev AA, et al. (2002) Late Pleistocene and Holocene vegetation and climate on the Taymyr lowland, Northern Siberia. *Quat Res* 57:138–150.
7. Hubberten HW, et al. (2004) The periglacial climate and environment in northern Eurasia during the Last Glaciation. *Quat Sci Rev* 23:1333–1357.
8. Stuart AJ (1999) *Late Pleistocene Megafaunal Extinctions* (Kluwer Academic/Plenum Publishers, New York).
9. Thieme H (1997) Lower Palaeolithic hunting spears from Germany. *Nature* 385: 807–810.
10. Stuart AJ (1991) Mammalian extinctions in the Late Pleistocene of northern Eurasia and North America. *Biol Rev Camb Philos Soc* 66:453–562.
11. Kutzbach J, et al. (1998) Climate and biome simulations for the past 21,000 years. *Quat Sci Rev* 17:473–506.
12. Fiedel S, Haynes G (2004) A premature burial: comments on Grayson and Meltzer's "Requiem for overkill". *J Archaeol Sci* 31:121–131.
13. Shapiro B, et al. (2004) Rise and fall of the Beringian Steppe Bison. *Science* 306: 1561–1565.
14. Weinstock J, et al. (2005) Evolution, systematics, and phylogeography of Pleistocene horses in the New World: A molecular perspective. *PLoS Biol* 3:e241.
15. Barnes I, et al. (2007) Genetic structure and extinction of the woolly mammoth, *Mammuthus primigenius*. *Curr Biol* 17:1072–1075.
16. Debruyne R, et al. (2008) Out of America: Ancient DNA evidence for a New World origin of Late Quaternary woolly mammoths. *Curr Biol* 18:1320–1326.
17. Vereshchagin NK (1971) Prehistoric hunting and the extinction of Pleistocene mammals in the USSR. *Proceedings of the Zoological Institute of the USSR Academy of Sciences* 69:200–232.
18. Kuznetsova TV, Sulerzhitsky LD, Siegert C, Schirmer L (2001) New data on the "mammoth" fauna of the Laptev Shelf Land (Arctic Siberia). *The World of Elephants*, eds Cavarretta G, Giola P, Mussi M, Palombo MR. Roma, 16–20 October 2001, pp 289–292.
19. Grayson DK, Meltzer DJ (2003) A requiem for North American overkill. *J Archaeol Sci* 30:585–593.
20. Groves P (1997) Intraspecific variation in mitochondrial DNA of muskoxen, based on control region sequences. *Can J Zool* 75:568–575.
21. Holm LE, Forchhammer MC, Boomsma JJ (1999) Low genetic variation in muskoxen (*Ovibos moschatus*) from western Greenland using microsatellites. *Mol Ecol* 8: 675–679.
22. Mikko S, Roed K, Schmutz S, Andersson L (1999) Monomorphism and polymorphism at Mhc DRB loci in domestic and wild ruminants. *Immunol Rev* 167:169–178.
23. Depaulis F, Orlando L, Hänni C (2009) Using classical population genetics tools with heterochronous data: Time matters! *PLoS One* 4:e5541.
24. MacPhee RDE, Tikhonov AN, Mol D, Greenwood AD (2005) Late Quaternary loss of genetic diversity in muskox (*Ovibos*). *BMC Evol Biol* 5:49.
25. Mangerud J, Astakhov VI, Murray A, Svendsen JJ (2001) The chronology of a large ice-dammed lake and the Barents-Kara Ice Sheet advances, Northern Russia. *Global Planet Change* 31:321–336.
26. Mangerud J, et al. (2004) Ice-dammed lakes and rerouting of the drainage of northern Eurasia during the Last Glaciation. *Quat Sci Rev* 23:1313–1332.
27. Meldgaard M, Bennike O (1989) Interglacial remains of caribou (*Rangifer tarandus*) and lemming (*Dicrostonyx torquatus*?) from North Greenland. *Boreas* 18:359–366.
28. Funder S, Hansen L (1996) The Greenland ice sheet—a model for its culmination and decay during and after the last glacial maximum. *Bull Geol Soc Den* 42:137–152.
29. Lemey P, Rambaut A, Drummond AJ, Suchard MA (2009) Bayesian phylogeography finds its roots. *PLoS Comput Biol* 5:e1000520.
30. Minin VN, Bloomquist EW, Suchard MA (2008) Smooth skyride through a rough skyline: Bayesian coalescent-based inference of population dynamics. *Mol Biol Evol* 25:1459–1471.
31. Drummond AJ, Rambaut A, Shapiro B, Pybus OG (2005) Bayesian coalescent inference of past population dynamics from molecular sequences. *Mol Biol Evol* 22:1185–1192.
32. Vibe C (1967) *Arctic Animals in Relation to Climatic Fluctuations* (CA Reitzel, Denmark).
33. Lent PC (1978) Muskox. *Big Game of North America: Ecology and Management*, eds Schmidt J, Gilbert D (Stackpole Books, Harrisburg, Pennsylvania), pp 135–147.
34. Gunn A (1984) Aspects of the management of muskoxen in the Northwest Territories. *First International Muskox Symposium*, eds Klein DR, White RG, Keller S. Malloy (Lithographing, Ann Arbor, MI), pp 33–40.
35. Miller F, Russell R, Gunn A (1977) Distributions, movements and numbers of Peary caribou and muskoxen on western Queen Elizabeth Islands, Northwest Territories, 1972–1974. *Can Wildl Serv Rep Ser* 40:1–55.
36. Vibe C (1958) The musk ox in East Greenland. *Mammalia* 22:168–174.
37. Pitulko VV, et al. (2004) The Yana RHS site: Humans in the Arctic before the last glacial maximum. *Science* 303:52–56.
38. Gilbert MTP, et al. (2008) Intraspecific phylogenetic analysis of Siberian woolly mammoths using complete mitochondrial genomes. *Proc Natl Acad Sci USA* 105: 8327–8332.
39. Grootes PM, Stuiver M, White JWC, Johnsen S, Jouzel J (1993) Comparison of oxygen isotope records from the GISP 2 and GRIP Greenland ice cores. *Nature* 366:552–554.
40. Grootes PM, et al. (2001) The Taylor Dome Antarctic 18O record and globally synchronous changes in climate. *Quat Res* 56:289–298.
41. Sher AV, Kuzmina SA, Kuznetsova TV, Sulerzhitsky LD (2005) New insights into the Weichselian environment and climate of the East Siberian Arctic, derived from fossil insects, plants, and mammals. *Quat Sci Rev* 24:533–569.
42. Lent PC (1988) *Ovibos moschatus*. *Mamm Species* 302:1–9.
43. Pitulko V (2001) Terminal Pleistocene–Early Holocene occupation in northeast Asia and the Zhokhov assemblage. *Quat Sci Rev* 20:267–275.
44. Kuzmin YV, Tankersley KB (1996) The colonization of Eastern Siberia: an evaluation of the Paleolithic age radiocarbon dates. *J Archaeol Sci* 23:577–585.
45. Orlova LA, Kuzmin YV, Zolnikov ID (2000) Time-space systematics for mammoths (*Mammuthus primigenius* Blum.) and prehistoric humans in Siberia (on the basis of radiocarbon dating). *Archaeol Ethnol Anthropol Eurasia* 1:31–41.
46. Meldgaard M (1991) New perspectives on the zoogeography of the Greenlandic caribou (*Rangifer tarandus*). *4th North American Caribou Workshop*, eds Butler C, Mahoney SP (Newfoundland and Labrador Wildlife Division, St. John's, Newfoundland), pp 37–63.
47. Knuth E (1981) Greenland news from between 81° and 83° north. *Folk* 23:91–111.
48. Bennike O (1997) Quaternary vertebrates from Greenland: A review. *Quat Sci Rev* 16: 899–909.
49. Dawes P, Elander M, Ericson M (1986) The wolf (*Canis lupus*) in Greenland: A historical review and present status. *Arctic* 39:119–132.
50. Alley R (2000) The Younger Dryas cold interval as viewed from central Greenland. *Quat Sci Rev* 19:213–226.
51. Alley R (2004) *GISP2 Ice Core Temperature and Accumulation Data* (IGBP PAGES/World Data Center for Paleoclimatology NOAA/NGDC Paleoclimatology Program, Boulder, CO).
52. Gulløv HC (2004) *Grønlands Forhistorie* (Gyldendal, Copenhagen), pp 434.
53. Haile J, et al. (2009) Ancient DNA reveals late survival of mammoth and horse in interior Alaska. *Proc Natl Acad Sci USA* 106:22352.
54. Kolokotronis S-O, MacPhee R, Greenwood A (2007) Detection of mitochondrial insertions in the nucleus (NuMts) of Pleistocene and modern muskoxen. *BMC Evol Biol* 7:67.
55. Ronquist F, Huelsenbeck JP (2003) MrBayes 3: Bayesian phylogenetic inference under mixed models. *Bioinformatics* 19:1572–1574.
56. Posada D, Crandall KA (1998) MODELTEST: testing the model of DNA substitution. *Bioinformatics* 14:817–818.
57. Rambaut A, Drummond A (2004) Tracer 1.4 (Available from <http://tree.bio.ed.ac.uk/software/tracer>). Accessed September 1, 2008.
58. Drummond AJ, Rambaut A (2007) BEAST: Bayesian evolutionary analysis by sampling trees. *BMC Evol Biol* 7:214.
59. Axelsson E, Willerslev E, Gilbert MTP, Nielsen R (2008) The effect of ancient DNA damage on inferences of demographic histories. *Mol Biol Evol* 25:2181–2187.
60. Ho SYW, Heupink TH, Rambaut A, Shapiro B (2007) Bayesian estimation of sequence damage in ancient DNA. *Mol Biol Evol* 24:1416–1422.
61. Rambaut A, Ho SYW, Drummond AJ, Shapiro B (2009) Accommodating the effect of ancient DNA damage on inferences of demographic histories. *Mol Biol Evol* 26: 245–248.
62. Suchard MA, Weiss RE, Sinsheimer JS (2001) Bayesian selection of continuous-time Markov chain evolutionary models. *Mol Biol Evol* 18:1001–1013.
63. Anderson CNK, Ramakrishnan U, Chan YL, Hadly EA (2005) Serial SimCoal: A population genetics model for data from multiple populations and points in time. *Bioinformatics* 21:1733–1734.
64. Excoffier L, Novembre J, Schneider S (2000) SIMCOAL: a general coalescent program for the simulation of molecular data in interconnected populations with arbitrary demography. *J Hered* 91:506–509.
65. Lemey P, Rambaut A, Drummond AJ, Suchard MA (2009) Bayesian phylogeography finds its roots. *PLoS Comput Biol* 5:e1000520.